Materials Science and Engineering B 273 (2021) 115392

Contents lists available at ScienceDirect

Materials Science & Engineering B

journal homepage: www.elsevier.com/locate/mseb

Changes in electrical properties and conduction mechanisms of Pd/n-Si diodes due to niobium dopant

M.J. Thebe [a], S.J. Moloi [b,*], M. Msimanga [c]

[a] Department of Physics, Vaal University of Technology, Private Bag X 021, Vanderbijlpark 1911, South Africa
[b] Department of Physics, University of South Africa, Private Bag X 6, Florida 1710, South Africa
[c] Department of Physics, Tshwane University of Technology, Private Bag X 680, Pretoria 0001, South Africa

ARTICLE INFO

Keywords:
Silicon
Schottky diodes, current
Capacitance
Resistivity

ABSTRACT

A change in electrical properties of silicon (Si) diodes due to niobium (Nb) doping was studied using current–voltage (*I-V*) and capacitance–voltage (*C-V*) techniques. The observed ohmic *I-V* behaviour and a low-voltage capacitance peak on Nb-doped Si diodes indicated that a charge distribution mechanism has been changed and dominated by generation-recombination defect centres in the material. These Nb-induced defect centres are responsible for a reduction in free majority carrier density in the space charge region as a result of charge compensation hence an increase in material resistivity. An increase in material resistivity is confirmed by relatively high series and shunt resistances evaluated on Nb-doped Si diodes. Furthermore, the effects of Nb doping on other diode parameters such as the saturation current, Schottky barrier height, ideality factor and doping density were investigated in the study. Since the observed diode property changes are similar to those induced by promising dopants for silicon radiation-hardness, the results presented here would, therefore, assist in a quest to improve radiation-hardness of silicon by defect-engineering strategy.

1. Introduction

Studies on metal-doped silicon (Si) have been carried to tune material properties for the fabrication of the improved radiation-hardness material-based sensors [1–3]. The tuning of material properties is necessary since the sensors are damaged by the same radiation they intend to sense [4]. As an elemental semiconductor, Si is a relatively defect-free semiconductor making its properties be easily understood, hence easily be tuned for various applications. In Si metals may induce defects with properties similar to those of radiation, hence render the material useless for the fabrication of radiation sensors. Therefore, studies on a change in Si properties due to metal doping is important to maximize favourable effects of metals in the material.

Lithium was proposed to be a suitable dopant to improve properties of Si for radiation sensing applications [1]. A possibility to tune material properties for radiation sensing applications was later reported based on the data acquired from the diodes fabricated on gold (Au)- and platinum (Pt)- doped Si [2]. Due to doping, all Si vacancies become occupied by dopant atoms inhibiting a charge generation or recombination by radiation. Thus, material properties become independent of incident radiation and no further degradation occurs when the detector is under operation. The improvement of Si radiation-hardness can also be achieved by initial heavy irradiation of the material [5–6]. Though metal doping and heavy irradiation are promising for radiation-hardness of the material, their effects on electrical properties of the material-based devices have not been fully understood nor explained. In addition, devices fabricated on the metals (Au and Pt) -doped [7] and irradiated [6] material have high leakage current resulting in a low detection sensitivity during operation. Both Au and Pt are relatively expensive making a study on defect-engineered Si for radiation sensing applications challenging. A search for alternative dopants to improve Si properties, as a result, is important. Studies on a change in electrical properties of the diode due to the dopants is important for fabrication of efficient radiation sensors to meet the requirements for the current and future demands [4,8,9].

In Si Nb has been used to improve properties of the material for applications in the modern microelectronic industry. Nb induces donor levels at $E_C - 0.26$ eV and $E_V + 0.4$ eV in the energy gap of Si [10] and at $E_C - 0.293$ eV and $E_V + 0.163$ eV [11]. A conclusive evidence of properties of Nb-induced defect level at $E_C - 0.583$ eV, close to Si mid-energy gap, however, could not be provided [11]. A defect level at $E_C - 0.570$ eV, very close to $E_C - 0.583$ eV, was also reported based on

* Corresponding author.
E-mail address: moloisj@unisa.ac.za (S.J. Moloi).

https://doi.org/10.1016/j.mseb.2021.115392
Received 3 November 2020; Received in revised form 11 June 2021; Accepted 6 August 2021
Available online 25 August 2021

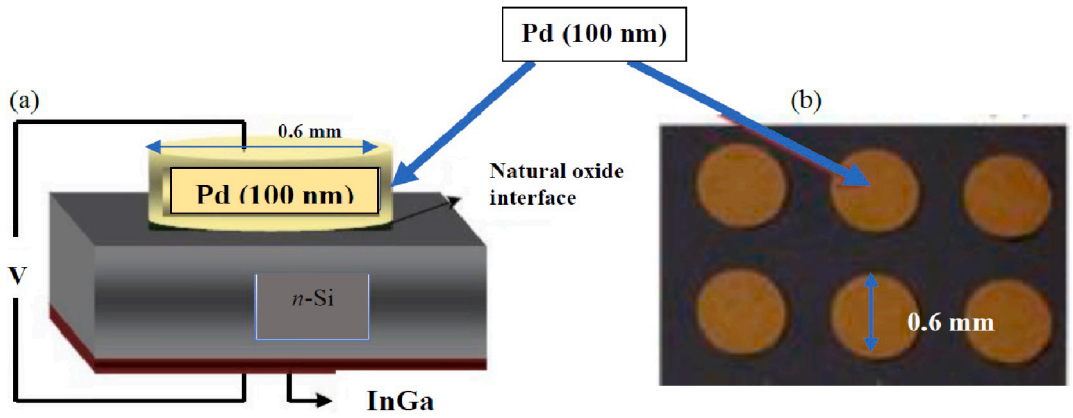

Fig. 1. Schematic diagram showing Pd/n-Si Schottky diodes (a) and circular Schottky contacts (top surface) (b).

the data acquired on Si implanted with Nb to the fluences of 1×10^{11} cm^{-2} and 3×10^{11} ion.cm^{-2} [12]. At the higher fluence of 1×10^{12} ion.cm^{-2}, Nb induces additional defect level at Si mid-energy gap, $E_C - 0.55$ eV [12]. This mid-energy gap defect level in Si is induced by heavy metals, Au [13] and Pt [14], and neutron irradiation [15]. Devices fabricated on the material rich of mid-energy gap defect levels show ohmic *I-V* behaviour and they have high electric resistivity due to a charge recombination activity by these levels in Si [3,6–9,15,16].

This work presents the effects of Nb doping on the electrical properties of Si diodes. The study was motivated by the reported Nb-induced defect level at $E_C - 0.55$ eV in the energy gap of Si [12]. The results obtained in this work show, for the first time, that Nb in Si exhibits similar properties as those of the metals (Au and Pt) and radiation and it could be an alternative dopant in a study to improve electrical properties of the material for radiation sensing applications.

2. Experimental details

2.1. Material preparation

Niobium was implanted onto the front (or polished) side of Si pieces at an energy of 160 keV and a nominal dose of 3×10^{15} ion.cm^{-2} was achieved. The resistivity of Si (111) oriented wafer was quoted by the manufacturer as 1–20 Ω.cm and the thickness as 275 ± 25.0 μm. Prior to implantation, Transport of Ions into Matter (TRIM) simulations were used to predict the penetration depth of the implantation energy of 160 keV.

The wafer was diced into 0.5 cm × 0.5 cm pieces using a laser cutter. The substrates were cleaned with an ultrasonic cleaner, successively using methanol, acetone, trichloroethane and de-ionized water to remove any dirt and handling grease. 40 % HF solution was used to etch a Si surface oxide layer. After the cleaning process, two pieces were mounted in the chamber for niobium implantation. The implantation was carried out using a 350 D Varian ® ion implanter set up at iThemba LABS, (TAMS), South Africa.

2.2. Diode fabrication

Diodes were fabricated on unimplanted and Nb-implanted *n*-type crystalline Si. Prior to diode fabrication, Si pieces were cleaned again using the same procedure described above before being loaded into an evaporation system for formation of Schottky contacts. The contacts were achieved by vacuum evaporation and deposition of 100 nm palladium (Pd) through a mask with 0.6 mm diameter holes. The deposition was carried out in a vacuum of 10^{-6} mbar to minimize the interface oxide layer at the rate of 1 Å.s^{-1}. The ohmic contact was then realised by rubbing indium galinide (InGa) onto the back (unpolished) surface of the pieces. The finished devices each consisted of 16 diodes on a piece with one common ohmic contact. The schematic diagram of the

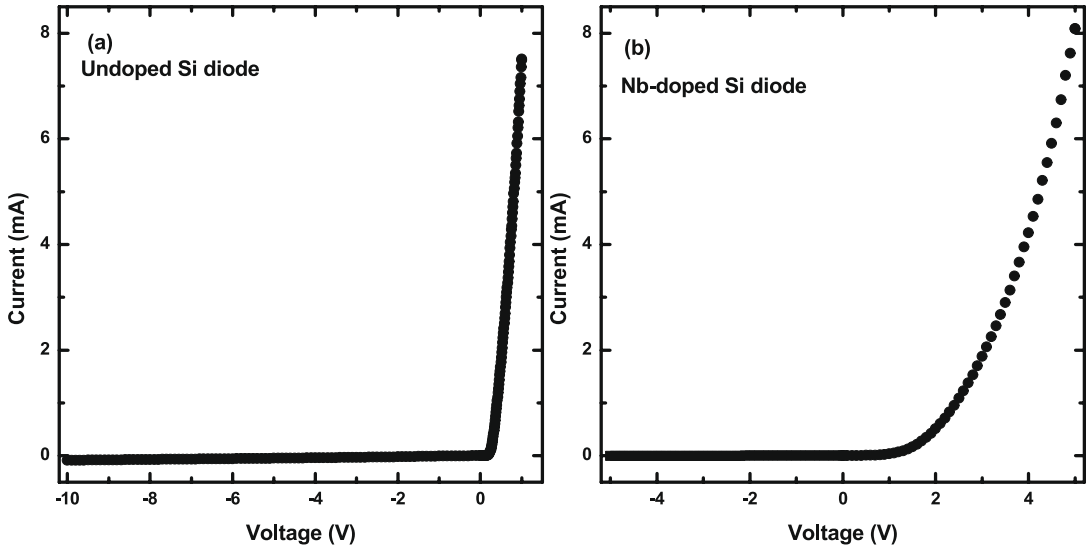

Fig. 2. I-V characteristics of the diodes fabricated undoped and Nb-doped n-Si diodes in linear scale. The measurements were carried out in the dark and at room temperature.

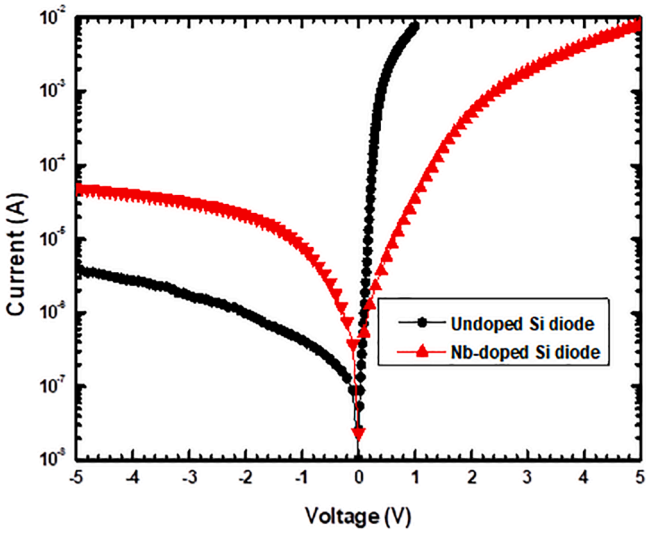

Fig. 3. . Forward and reverse bias semi-logarithmic I-V characteristics of the diodes fabricated on undoped and Nb-doped n-Si in the dark and at room temperature.

fabricated diodes is shown in Fig. 1.

2.3. Device characterisation

Devices in this work are Schottky diodes that were fabricated on undoped and Nb-doped Si. All the characterisations were carried out at room temperature. The diodes were characterised by *I-V* technique using Keithley 6487 picoammeter with a voltage source. For the current measurements, the data was acquired at the voltage range, −4 to 1 V for diodes fabricated on undoped Si, while the range of −10 to 5 V was used for diodes fabricated on Nb-doped Si. The difference in voltage measurement ranges is based on the data that was presented before on the diodes that were fabricated on defected material [7,16]. The forward current was found to tilt toward the voltage-axis making the current limit to be reached at voltage higher than relatively defect-free material-based diodes.

Capacitance measurements with the diodes connected in reverse bias were carried out at frequencies of 1 MHz and 120 kHz, using HP 4192 LF analyser and Agilent 4263B LCR meter, respectively. The measurements were carried out at voltage range of 0–6 V for 1 MHz and of the 0–30 V range for 120 kHz. Since the LCR meter does not have a built-in voltage source, the voltage was applied to the devices under test driven from Keithley 6487 picoammeter. A MATLab programme was written using M-File codes for interface of Picoammeter and LCR meter and for data acquisition.

3. Results and discussion

Fig. 2 shows *I-V* characteristics of the fabricated diodes in linear–-linear scale. *I-V* measurements were carried out on six diodes fabricated on each material (undoped and Nb-doped *n*-Si) and they showed similar rectifying behaviour as observed in the figure. As expected, the reverse current is completely independent of voltage in this scale since the reverse current is due to minority carriers (holes) in *n*-Si. In forward bias, a switch-on voltage is observed at 0.25 V for undoped and at 1.5 V for Nb-doped Si diodes. A delayed switch-on voltage with less abrupt forward current increase observed in Fig. 2 (b) indicates that higher energy is required to have high density of free charge carriers withdrawn to the opposite electrodes to contribute to the measured current. Both trends in Fig. 2 indicate that the diodes were well fabricated and obey a well-known semiconductor diode equation [17–19],

Table 1
Diode parameters calculated using lnI-V and dV/dlnI - I methods.

	ln*I-V*			d*V*/dln *I* - *I*	
Si diode	I_s (nA)	Φ_{IV} (eV)	η	η	R_s (Ω)
Undoped	4.30±1.40	0.71±0.01	1.20±0.04	1.55±0.02	23±0.06
Nb-doped	1192±2.26	0.62±0.02	11.9±5.35	1.12±2.01	98.72±0.20

$$I = I_S\left[\exp\left(\frac{eV}{\eta kT} - 1\right)\right] \quad (1)$$

where I_S is the saturation current, e is the electronic charge, V is the applied voltage, η is the ideality factor, k is the Boltzmann's constant and T is the temperature.

The rectifying behaviour of the fabricated diodes is confirmed by semi-logarithmic *I-V* behaviour of the diode presented in Fig. 3. The reverse current shows a weak voltage dependence and a non-saturation behaviour possibly due to the presence of a native interfacial layer between Pd and Si. The forward current increases linearly and deviates at high voltage because of series resistance and interface states on the properties of the diodes [20,21]. The saturation current, I_S, is determined from the intercept of semi-logarithmic forward biased *I-V* plot at the voltage greater than $3kT/e$ as

$$I_S = AA^*T^2\left(\frac{-e\Phi_{IV}}{kT}\right) \quad (2)$$

where A is the diode area, A^* is the Richardson constant (=112 A-cm^{-2}-K^{-2}) for *n*-type Si,Φ_{IV} is the Schottky barrier height given as

$$\Phi_{IV} = \frac{kT}{e}\ln\left(\frac{AA^*T^2}{I_S}\right) \quad (3)$$

The ideality factor for both diodes was obtained from the slope of the forward linear regions in Fig. 3 as

$$\eta = \frac{q}{kT}\left(\frac{dV}{d(\ln I)}\right) \quad (4)$$

The average saturation current for six undoped Si-based diodes was evaluated to be (4.3 ± 1.4) nA. Tunc *et al.* [22], on the other hand, reported a value of 2.7 nA, which is lower than the one reported in this work. A high value of 8400 nA was reported based on Au/*n*-Si diodes [7]. All these saturation currents were extracted from Si substrate with different metals for Schottky contacts. The saturation current evaluated in this work is within the range of those evaluated by other researchers confirming that the diodes for this work were well fabricated [7,22].

The saturation current evaluated on Nb-doped Si diode is, 1192±2.26 nA, higher than 4.30 ±1.40 nA, evaluated on undoped Si diode (Table 1). An increase in the saturation current indicates that Nb has induced crystal lattice defects that trap free charge carriers (majority carriers) resulting in a decrease in carrier density through the space charge region (SCR), hence an increase in reverse current (Fig. 3). The reverse current for Nb-doped Si diode is higher than that of undoped Si diode for the whole voltage range indicating that Nb-induced defects have been extended in the bulk of Si. The induced defects are responsible for generation of minority carriers (holes) in the bulk and near SCR to compensate the majority carriers hence increase the resistivity of Si [9].

A reduction of free charge carrier density is confirmed by relatively low forward current observed on Nb-doped Si diode in Fig. 3. The rectification ratio, a ratio of forward current to reverse current at 1 V, for undoped and Nb-doped Si diodes is greater than unity and was evaluated as $\sim 31.5 \times 10^3$ and ~ 4.63, respectively indicating that the conductivity for both diodes is dominated by majority carriers. A decrease in the rectification ratio has been reported based on neutron irradiated Si diodes [9]. A decrease in rectification ratio is due to a decrease

(increase) in the density of majority (minority) charge carriers [9]. This variation of the density implies that in *n*-Si, the electrons are compensated/recombined with Nb generated minority carriers (holes) to increase the reverse current as observed in Fig. 3.

The evaluated mean Schottky barrier height for undoped Si-base diodes is 0.71 eV, the same as the one evaluated on Pb/*n*-Si diode [23]. Horvath *et al.* [24] reported the Schottky barrier height of 0.76 eV on Al/*n*-Si diode while Tunc *et al.* [22] reported 0.747 eV on Au/PVA (Co,Ni-doped) *n*-Si diodes. Though these values are higher than the one obtained in this work they can be used for comparison purposes.

The evaluated Schottky barrier height is, however, lower than the theoretical value of 1.05 eV confirming the existence of states at Pd/*n*-Si interface. This theoretical value was calculated using the relation, $\Phi_{IV} = \Phi_m - \chi$, where Φ_m is the Palladium work function (5.12 eV) and χ is the electron infinity of Si (4.05) [19]. It has been reported that a silicon oxide layer of 1–3 nm thick would always be found on the surface even after etching Si wafers with HF solution [25]. The interface layer may be formed either during material preparation or during device fabrication processes. This layer affects the practical Schottky barrier height. Furthermore, etching with HF may affect the roughness of the surface, hence the quality of the diodes and the evaluated parameters. This roughness may also result in a difference in Schottky barrier height and other parameters. The effects of surface roughness are, however, common for both types of diodes (undoped and Nb-doped Si diodes) since they were fabricated in the same conditions. Hence, a change in device properties presented in this work is assumed to be only due to Nb doping since it is the factor that makes the fabricated diodes different.

The mean Schottky barrier height evaluated on Nb-doped Si is ~ 0.62 eV, lower than the one evaluated for undoped *n*-Si diode. There are various reasons for a decrease in the barrier height in the literature. Possible explanations are the presence of interface states [26] and reduction of the carrier density in SCR [27]. It has to be noted that both diodes were prepared in the same conditions hence a change in diode properties due interface states could be insignificant. Though it is affected by metal–semiconductor interface, a decrease in barrier height is due to Nb doping. It is also possible that Si surface roughness could be affected by high energy Nb implantation resulting in a change in the barrier height. The roughness of Si surface, therefore, may impact the Schottky barrier height, making the parameter more of a surface than a bulk property.

As it penetrates Si, Nb loses its energy due to atomic nuclear and electron cloud interactions. The calculated nuclear energy loss and electronic energy loss are 92.0 % and 62.8 %, respectively indicating that the nuclear part is the dominant mechanism of the energy loss per unit length in Si. The interaction of Nb with Si atoms results into lattice defects in the path from the surface into the bulk of Si. The Nb-induced defects generate minority carriers to compensate majority carriers hence increase in the leakage current (Fig. 3) and the saturation current (Table 1). The density of free charge carrier in SCR decreases.

The mean ideality factor of undoped Si diode is found to be 1.20 very close to 1.12 and 1.17 evaluated on Au/*n*-Si diode with 1.5 nm and 2.5 nm metal-silicon interfacial layer thickness, respectively [28]. The evaluated ideality factor indicates that there is a thin interfacial layer between Pd and Si. The ideality factor, however, is lower than 1.4 evaluated by Msimanga *et al.* [7] on Au/*n*-Si diode. The ideality factor of undoped *n*-Si diodes evaluated in this work is within the range (1.12–1.196) of those found in the literature [7,28] indicating that the diodes were well fabricated using Pd for Schottky contact. The average ideality factor of diodes fabricated on Nb-doped Si far exceeds unity and is evaluated to be 11.9. The ideality factor higher than 2 has been reported before and was attributed to other current flow mechanisms than thermionic emission [9,26,29–30]. The ideality factor of 496 was evaluated on the commercial Si diode irradiated by neutrons to a fluence of 10^{16} n cm^{-2} [9]. This high value might be an indication that there are defects induced on the surface of the material to cause the tunnelling behaviour.

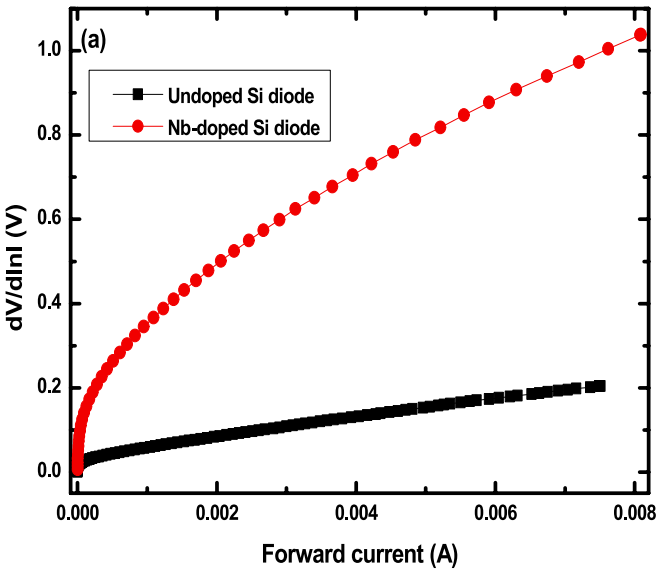

Fig. 4. dV/dlnI-I characteristics of the the diodes fabricated on undoped and Nb-doped n-Si in the dark and at room temperature.

The effects of series resistance are observed by flattening of the forward current trends at high voltage in Fig. 3 and it can be calculated using Cheung and Cheung method [31] as

$$\frac{dV}{d(\ln I)} = \left(\frac{\eta kT}{q}\right) + IR_s. \quad (5)$$

Fig. 4 presents $\frac{dV}{d(\ln I)}$ - *I* plots of undoped and Nb-doped Si diodes. The slope of the linear region gives R_s and the intercept on the *y*-axis is used to evaluate the ideality factor. The values of η and R_s are presented in Table 1. Values of the ideality factor evaluated using ln*I*-*V* and Cheung's method are different from each other due to the distinct linear forward current regions they are evaluated from [32]. In the case of ln*I*-*V* method the parameters are evaluated at low voltage range where the effect of R_s on *I*-*V* characteristics is less significant.

The value of ideality factor evaluated on Nb-doped diode is lower than that evaluated on undoped Si using Cheung's method and it is closer to the ideal Schottky diode unity. This low ideality factor evaluated for this diode probably indicates that η is less dependent on the defects induced in the material hence less pronounced when the diode conduction mechanisms is dominated by charge distribution in the bulk. Ideality factors for both diodes are however still higher than unity indicating that there are diode conduction mechanisms other than thermionic emission. A high R_s evaluated on Nb-doped Si diode indicates a reduction of free charge carrier density in SCR. This reduction is due to compensation of the charge carriers in the region showing that the Nb-induced defects are responsible for generation of holes in the material.

The forward bias logarithmic plots for both diodes were generated and presented in Fig. 5 to study a change in diode conduction mechanism due to Nb doping. Two distinct linear regions with different slopes for undoped Si diode and three distinct linear regions for Nb-doped diodes are observed in forward bias. The plots for both diodes show a power law behaviour between the current and applied voltage with different values of exponent (slopes). In the low forward voltage range, the region $(0.1 < \log V < 0.45)$ gives a slope of 5.56 and of 2.2 in the high voltage range for undoped Si diodes. Slopes higher than two is an indication of trapped-charge-limited current (TCLC) with an exponent trap distribution [33,34]. The diode conduction mechanisms in this case could be governed by the space charge limited current (SCLC) with exponentially distributed surface states for undoped Si diode [33,34]. In SCLC mechanisms, the injection of electron from the electrodes to the

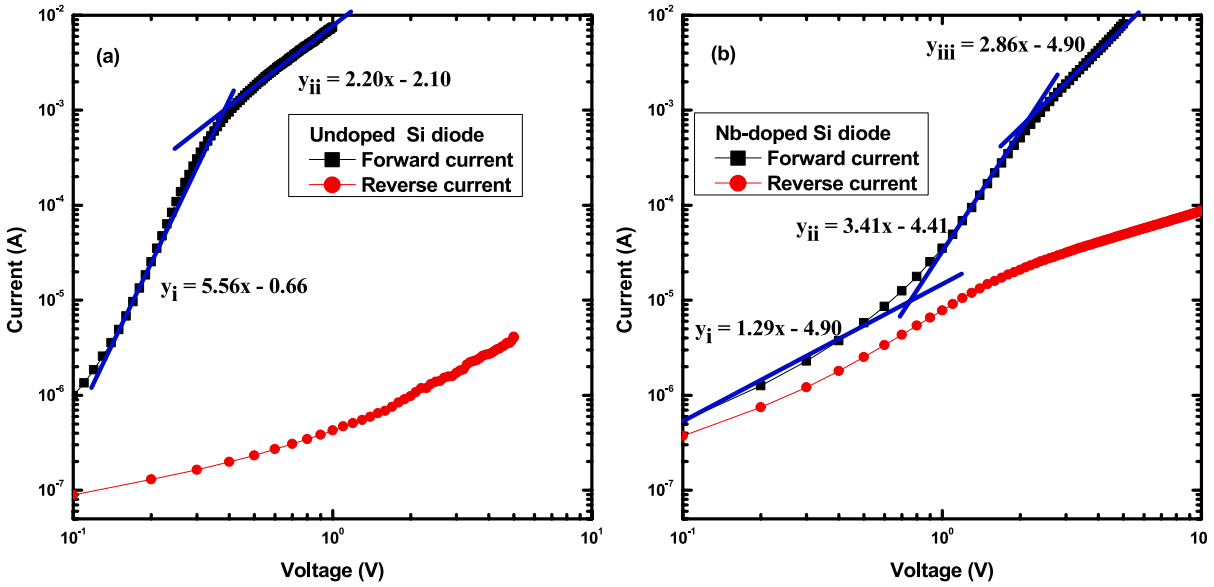

Fig. 5. The double logarithmic I-V plots for the diodes fabricated on undoped and Nb-doped n-Si in the dark and at room temperature. Blue solid lines define the different linear regions of the plots. (For interpretation of the references to colour in this figure legend, the reader is referred to the web version of this article.)

region increases with voltage.

Three linear regions with different slopes in forward current of Nb-doped Si diode are observed in Fig. 5 (b). The evaluated slope in the first region is, 1.29, close to unity, indicating that the dominant conduction mechanism is ohmic. This ohmic behaviour is attributed to the domination of the generated current in SCR over the injected free carrier generated current [33,34]. The injected carrier density may be lower than the background thermal carrier density [33,34]. Thus, the density of the injected carrier from the material to SCR has decreased after Nb-doping. This reduction in the density is due to recombination/compensation of free charge carriers by minority carriers that are generated by Nb-induced defect levels in the material.

A decrease in free carrier density in SCR can be interpreted in terms of a change in the magnitude of current trends at high voltages. It can be seen from Fig. 5 that the forward current has decreased by a factor of $\sim 3 \times 10^2$ while the reverse current has increased by a factor of 2×10^1 at 1 V after doping with Nb. This change in currents confirms that the free carrier density decreases at the rate higher than the rate in which minority carrier density increases after Nb doping. The results indicate that Nb-induced defect levels are responsible for generation of minority carriers that recombine charge carriers to decrease the forward current hence increase the resistivity of the material.

The effects of these generation-recombination (*g-r*) centres can be explained by the forward and reverse current trends in Fig. 5 (b) being parallel and close to each other especially, at low voltages, to show the diodes have changed from typical exponential to ohmic behaviour after doping Si with Nb. Similar trends have been observed before on the diodes fabricated on Au-doped [9] and on Pt-doped Si [16]. The behaviour was also observed on the irradiated Si diodes and was explained in terms of midgap defects [6,15], defects that are positioned at the centre of the energy gap (~0.56 eV). The effects of radiation damage on the diodes exhibiting ohmic behaviour are suppressed [6]. The Fermi energy of the material rich of *g-r* centres is pinned at the intrinsic-position and at this position it is not affected by incident particle [35]. *g-r* centres interact with both bands such that charge carrier generation rate (*g*) is the same as recombination rate (*r*) making the diode behaviour ohmic. Both minority and majority carriers are injected

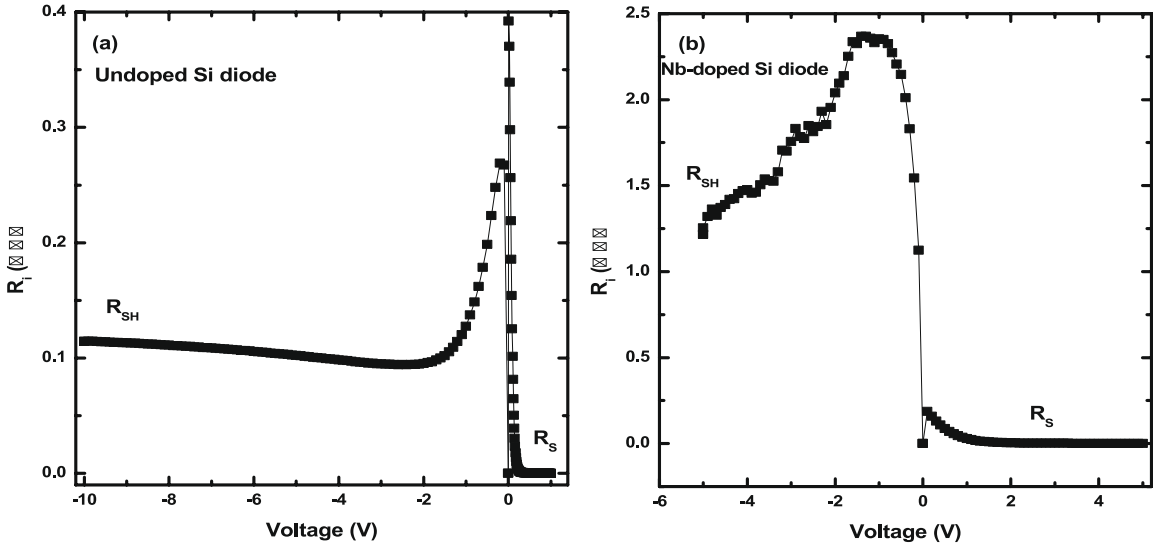

Fig. 6. The voltage dependent device resistance of the diodes fabricated on 1undoped and Nb-doped n-Si in the dark and at room temperature.

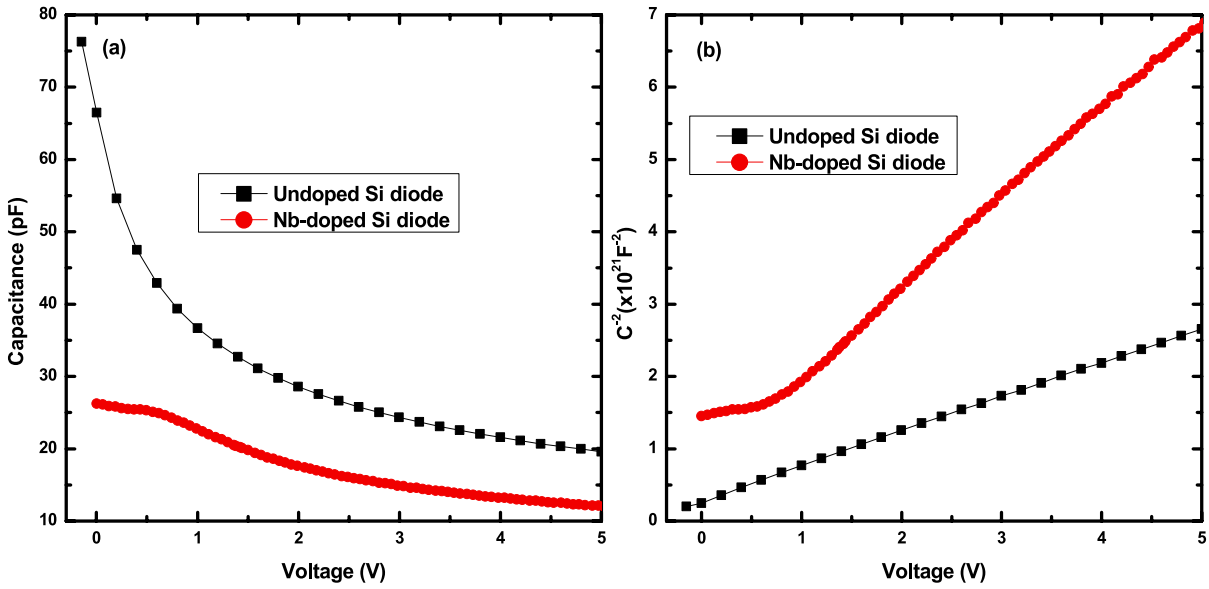

Fig. 7. C-V (a) and C^{-2}-V (b) characteristics of the diodes fabricated on undoped and Nb-doped n-Si in the dark and at room temperature.

at the same rate and recombining each other in SCR hence reduction in free charge carrier density contributing to the measured current.

To have an in-depth knowledge about a change in the device properties due to Nb- doping, the R_s and shunt resistance (R_{SH}) were determined from the plots of diode resistance (R_i) against voltage, where $R_i = \partial V/\partial I$, is determined from the *I-V* characteristics and the plots are shown in Fig. 6. As the forward bias increases, R_i decreases and becomes constant at certain value, which gives R_s [36]. Values of R_s evaluated using the plots in Fig. 6 for undoped and Nb-doped Si diodes are 140.74 and 643.04 MΩ, respectively. Though these values of R_s are much higher than those presented in Table 1, both methods indicate that R_s increases by a factor of ~ 4.4 due to Nb doping confirming a decrease in free charge carrier density in SCR.

In reverse bias, on the other hand, the maximum value of R_i corresponds to R_{SH} which is found to be 0.28 and 2.36 MΩ for undoped and Nb-doped Si diodes, respectively. After this maximum value, the R_i trends decrease with voltage for both diodes. The trend in Fig. 6 (a) decreases drastically with negative voltages to R_i of 0.11 MΩ at 1.5 V to show high injection rate of charge carriers in SCR. This drastic decrease is expected since the material is void of defect levels responsible for recombination/compensation of free charge carriers. As the space charge region extends into the bulk, the R_i becomes independent of the voltage indicating that the resistivity in Si bulk is constant.

A gentle decrease in R_i with negative voltage for Nb-doped diode is observed in Fig. 6 (b) indicating a slow charge carrier injection rate in SCR. An absence of R_i saturation with the applied voltage in Fig. 6 (b) indicates that the induced defect density decreases with Nb penetration depth in the bulk. It is believed that the trend for Nb-doped Si diode would not decreases indefinitely. It is expected that at a certain voltage higher than −5 V R_i would be ~ 0.11 MΩ and then remain independent of the voltage. This voltage would be associated to the maximum penetration depth of ~ 92 nm which was estimated using TRIM calculations. The depth profile of the induced defects is, however, not the scope of this work.

Fig. 7 (a) shows *C-V* characteristics of the fabricated diodes. The observed steep fall in the capacitance at low voltages for undoped Si diode is an indication of an increase in SCR width with voltage. A gentle capacitance decrease at high voltage indicates that an increase in the SCR width is slow as the diodes attains its full depletion. Similar trends of diode capacitance have been observed before on diodes that were fabricated on Si material [27] on commercial *p-i-n* Si photodiodes [6]. Based on this observed typical *C-V* behaviour it can be deduced that the diodes were well fabricated.

C-V characteristics of the diodes fabricated on Nb-doped Si is markedly different from that of undoped Si diodes indicating a change in *C-V* properties after Nb doping. Three different regions are observed for *C-V* trend of Nb-doped Si diode. In the first region from 0 to 0.8 V, the capacitance is independent of the applied voltage showing that a charge carrier withdrawal rate from SCR is infinitesimal at this voltage range. It can also be observed in the figure that the capacitance has decreased for all voltages after Nb doping. A decrease in capacitance indicates a reduction of the free charge carrier density in SCR. As explained earlier using *I-V* data, the conduction mechanism at low voltage range for Nb-doped Si diode is dominated by *g-r* centres. These centres inject charge carriers in the same rate which then compensate each other in SCR. Due to high measurement frequency making low mobility minority carriers inactive, the injected majority carriers neutralize the existing ionized donors resulting in a decrease in charge carriers withdrawn from SCR. This charge neutralization makes capacitance independent of the voltage, as shown in the figure at low voltage range for Nb-doped Si diode. The effects of the induced *g-r* centres are clearly explained later in the text for a low frequency measurement, where the injected minority carriers are active in SCR.

In the intermediate region ~ 0.9 - ~ 2 V, a decrease in capacitance with voltage indicates that a considerable density of charge carriers is withdrawn from SCR. This decrease in capacitance for Nb-doped Si diode is not as rapid as that of undoped Si diode indicating that a charge carrier withdrawal rate has decreased after Nb doping. A decrease in the withdrawal rate indicates that minority carriers have been generated in Si to recombine/compensate free majority charge carriers to increase the resistivity of the material.

A SCR capacitance of Schottky diodes is given in terms of the applied voltage [27] as

$$C = A\sqrt{\frac{q\varepsilon_s\varepsilon_o N_D}{2(V_{bi}+V)}} \tag{6}$$

where ε_s (=11.8) is the dielectric constant of Si, ε_o is the dielectric constant of free space, N_D is the doping density and V_{bi} is the built-in voltage of the diode. The above equation can be simplified as

$$C^{-2} = \frac{2}{A^2}\mathrm{x}\frac{V_{bi}}{q\varepsilon_s\varepsilon_o N_D} + \frac{2}{A^2}\mathrm{x}\frac{V}{q\varepsilon_s\varepsilon_o N_D} \tag{7}$$

to show that N_D and V_{bi} is determined from the slope and the voltage

Table 2
Diode parameters evaluated from C-V plots at 1 MHz.

Si diode	Φ_{CV} (eV)	V_{bi} (eV)	ξ (keV. cm^{-1})	$\Delta\varphi$ (eV)	N_D ($\times 10^{15}$ cm^{-3})
Undoped	0.829 ± 0.02	0.60 ± 0.02	24.1 ± 0.41	0.01 ± 0.00	3.15 ± 0.04
Nb-doped	1.087 ± 0.17	0.84 ± 0.17	17.7 ± 1.80	0.01 ± 0.00	1.21 ± 0.05

intercept, respectively, of the linear plot of C^{-2} - V. The Schottky barrier height (Φ_{cv}) can then be computed [37–39] as

$$\Phi_{cv} = V_{bi} + \frac{k_B T}{q} \ln\left(\frac{N_C}{N_D}\right) - \Delta\varphi. \quad (8)$$

where Δφ is the potential barrier lowering due to the image charge induced in the Schottky barrier metal under the zero-bias condition and is defined in terms of the electric field at the interface, ξ, as

$$\Delta\varphi = \sqrt{\frac{q\xi}{4\pi\varepsilon_s\varepsilon_o}}. \quad (9)$$

The electric field, ξ, is given as

$$\xi = \sqrt{\frac{2q(N_D V_{bi})}{\varepsilon_s\varepsilon_o}}. \quad (10)$$

Fig. 7 (b) is C^{-2} – V plots to determine the doping profile and N_D for the fabricated diodes. The linear behaviour is observed for undoped Si diode indicating that the doping density is uniform in the material for the whole voltage range. Parameters evaluated from these diodes are given in Table 2. The evaluated mean Schottky barrier height is ~ 0.83 eV. Other parameters, V_{bi}, $\Delta\varphi$ and ξ were determined to evaluate the barrier height and are also presented in the table. Hanselaer *et al.* [28] found Φ_{CV} of 0.80 eV on Au/*n*-Si diode, which is close to 0.83 eV evaluated in this work. Said *et al.* [25], on the other hand, reported Schottky barrier heights of 0.860 eV, 0.881 eV and 0.896 eV on Au/*n*-Si diodes. The Schottky barrier height evaluated in this work is comparable to those obtained in the literature using *C-V* technique.

Φ_{CV} evaluated in this work is higher than Φ_{IV}. This discrepancy emanates from the nature of the techniques. Capacitance measurements are influenced by charge distribution at the SCR boundary which follows the weighted arithmetic average of the barrier heights [39]. In the current measurements, the current is dominated by charge carriers that flows through the region of low barrier height. Consequently, the barrier height measured using *I–V* technique is considerably lower than the weighted arithmetic average of the barrier heights. The *I-V* technique includes any barrier lowering effect due to interfacial oxide layer or interface states [38], thus resulting in lower barrier height values when compared to *C-V* measurements. Consequently, a meaningful comparison between Φ_{IV} and Φ_{CV} is impossible.

The mean doping density evaluated for the undoped Si diode is (3.15 ± 0.03) × 10^{15} cm^{-3}. This value of doping density is lower than the values of 4.0 × 10^{15} cm^{-3}, 6.3 × 10^{15} cm^{-3} and 10 × 10^{15} cm^{-3} reported by Hanselaer *et al.* [28] for the oxide interfaces thicknesses of 15, 24 and 25 nm, respectively, between Au and Si. The doping density evaluated in this work is higher than 0.7 × 10^{15} cm^{-3} determined by Msimanga *et al.* [7] on Au/*n*-Si diode. Doping density evaluated in this work is within the range of those reported in literature [7,28].

C^{-2} –V characteristic of Nb-doped Si diode has two linear regions as observed in Fig. 7 (b). There is a gentle increase of C^{-2} with voltage from 0 to 0.8 V which is followed by a linear increase from 1 to 6 V. Parameters that were evaluated from the wide linear region are given in Table 2. The evaluated mean of Schottky barrier height is ~ 1.1 eV, higher than (0.829 eV) obtained on undoped Si diodes. Though a comparison of Schottky barrier heights determined using current and capacitance measurements is meaningless, a comparison of variation of the parameters due to Nb doping for both techniques is very important. Explanation of this variation would lead to a clear understanding of change in electrical properties of the diodes due to Nb doping.

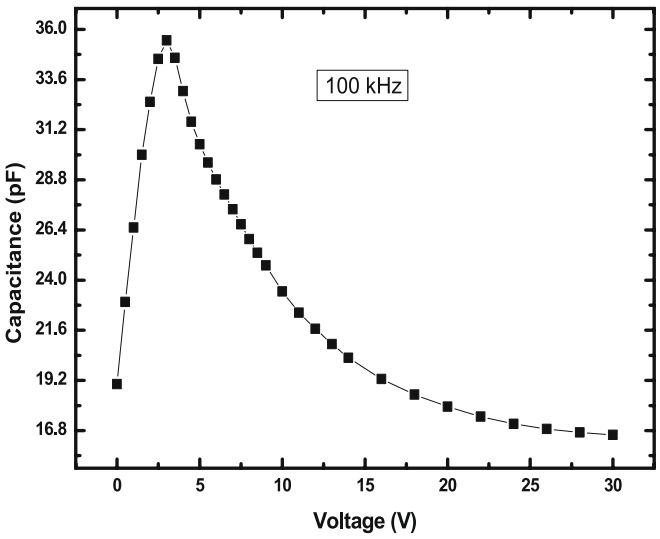

Fig. 8. C-V characteristic of a diode fabricated on Nb-doped n-Si measured at 100 kHz.

Unlike in *I-V* measurements where Φ_{IV} of Nb-doped Si diodes were evaluated to be lower than those of undoped Si diodes, in *C-V* measurements the opposite case holds. These results indicate that Schottky barrier heights determined from these techniques are incomparable and have different interpretations. Φ_{CV} is due to the density of charge carriers withdrawn to the opposite electrodes but not the density of charge carriers stored in SCR. Since for Nb-doped Si diode the charge carrier withdrawal rate is low, a high voltage is needed for high charge carrier density withdrawn to the opposite electrodes. Thus, an increase in Schottky barrier height due to Nb doping may explain the recombination/compensation of free charge carriers in SCR. This recombination/compensation activity results in a decrease of carrier density as confirmed by reduction of doping density from 3.15 × 10^{15}cm^{-3} to 1.21 × 10^{15}cm^{-3}.

The results obtained here show that the Schottky barrier height obtained from *I-V* measurements, on the other hand, is related to charge carrier density through SCR. The high charge carrier density through the region results in high saturation current. As a result, a low potential barrier is required for high charge carrier density withdrawn to the opposite electrodes. Φ_{IV}, therefore, explains the average charge carrier distribution mechanism in the material.

C-V measurements in reverse bias were also carried out on Nb-doped Si diode at low frequency, 100 kHz, and the results are shown in Fig. 8. Unlike in the case of high measurement frequency (1 MHz) in Fig. 7 (a), at low measurement frequency (100 kHz), low mobility injected minority carriers are also active and they have enough time to contribute to the conduction mechanism in SCR, hence increase in the capacitance of the material-based device.

At low voltage range, a peak, an initial increase of capacitance up to ~ 35 pF shows an increase in charge carrier density in SCR. At this voltage range (0–2.6 V) the conduction mechanism is dominated by Nb-induced *g-r* centres in Si. Since the injected minority carriers are active at this frequency, a high density of majority carriers (electrons) is required to have a charge neutrality state in SCR. The required density has increased in this case since at this measurement frequency the minority carriers that are injected in the same rate with the majority carriers are also active and together with ionised donors already present need to be compensated. As a result, the capacitance would initial increase due to this injected minority carriers till they get fully compensated. After being fully compensated, the majority carriers are then withdrawn from

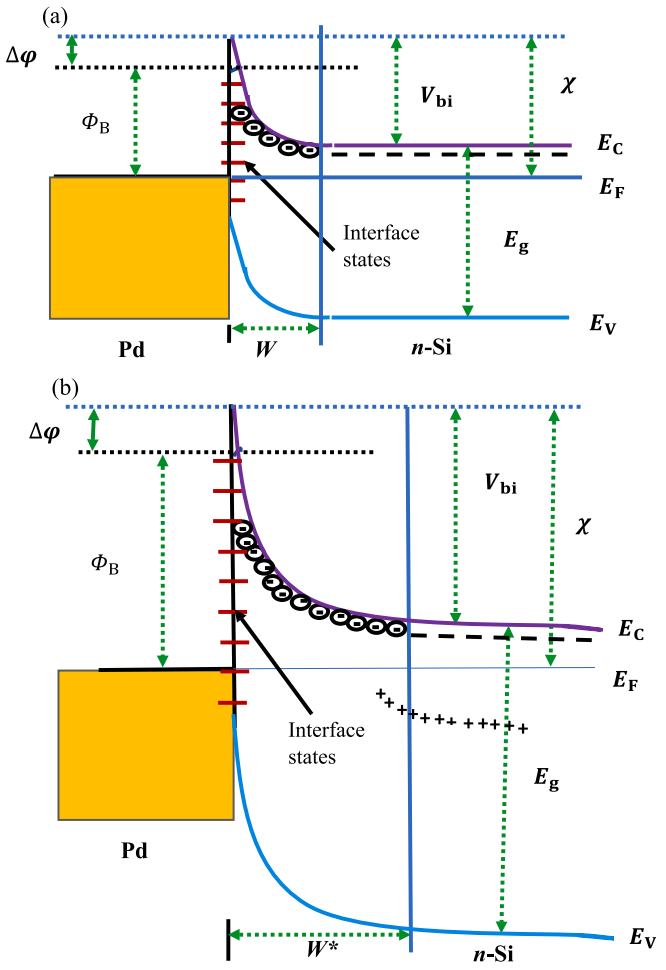

Fig. 9. Schematic energy band diagram of Pd/n-Si diodes in equilibrium for undoped n-Si (a) and Nb-doped n-Si (b). The symbols, ⊙⊙, - - - and + + + are ionized donors, donor levels and Nb-induced charged defect levels, respectively.

SCR resulting in a usual decrease in capacitance with voltage. Thus, a peak observed in Fig. 8 is due to *g-r* centres, defect levels that are positioned at the centres of the energy gap. At this position, *g-r* centres generate charge carriers that are injected at the same rate in SCR [6,7,15,16]. At low measurement frequency the effects of g-r centres are well interpreted since the minority carriers are mobile making the capacitance peak pronounced. A low-voltage capacitance peak observed in Fig. 8 was also observed on the diode that was fabricated on Au-doped *n*-Si [7] and on neutron irradiated Si *p-i-n* diodes [15].

The behaviour of the fabricated diodes possibly could be explained by a schematic diagram shown in Fig. 9. The figure shows the energy band diagrams of undoped and Nb-doped *n*-Si junctions with interface states between Pd and the material. The Nb-induced defect levels in the Si energy gap are responsible for recombination / compensation of the majority carriers resulting in a reduction of the charge carrier density in SCR. As observed from Fig. 9, a reduction in the carrier density causes a widening of SCR width from *W* to *W**.

4. Conclusion

Changes in *I-V* and *C-V* characteristics of Si diodes due to Nb doping were presented in this work. Both characterisation techniques complement each other showing that a charge distribution mechanism in the material changes and it is dominated by *g-r* centres after Nb doping. The effects of *g-r* centres were more pronounced at low-voltage range by ohmic *I-V* behaviour and the capacitance peak. These two features, ohmic *I-V* and the capacitance peak, indicate that the induced *g-r* centres are defect levels situated at the centre of the energy gap where they interact with both bands to maintain the Fermi energy at intrinsic position. As a result, charge carriers are injected in the same rate and recombine / compensate each other in SCR. The compensation of free charge carriers is confirmed by a decrease in forward current, while the generation of minority carrier for compensation is shown by an increase in reverse current. A diode fabricated on Nb-doped Si exhibits similar properties as those fabricated on Pt- and Au-doped and on heavily irradiated material. These diodes were later found to be resistant to radiation damage. This work, therefore, suggests that Nb is also a promising dopant to make silicon suitable for a study on fabrication of detectors to meet the current and future demands.

Declaration of Competing Interest

The authors declare that they have no known competing financial interests or personal relationships that could have appeared to influence the work reported in this paper.

Acknowledgements

We would like to thank Mr. Tony Miller of iThemba LABS for Nb implantation and Profs. D. Auret and M. Diale of the University of Pretoria for device fabrication and characterisation. This work is based on the research supported wholly by the National Research Foundation of South Africa (Grant numbers: 105292 and 114800).

References

[1] J.J. Wysocki, P. Rappaport, E. Davison, R. Hand, J.J. Loferski, Lithium-doped, radiation-resistant silicon solar cells, Appl. Phys. Lett. 9 (1) (1966) 44–46.
[2] R.L. Dixon, K.E. Ekstrand, Gold and platinum doped radiation resistant silicon diode detectors, Radiat. Prot. Dosim. 17 (1986) 527–530.
[3] M. McPherson, T. Sloan, B.K. Jones, Suppression of irradiation effects in gold-doped silicon detectors, J. Phys. D. Appl. Phys. 30 (21) (1997) 3028–3035.
[4] Y. Gurimskaya, P. Dias de Almeida, M.F. Garcia, et al., Radiation damage in p-type EPI silicon pad diodes irradiated with proton and neutrons, Nucl. Instr. Meth. Phys. Res. A 958 (2020), 162221.
[5] P.G. Litovchenko, A.A. Groza, V.F. Lastovetsky, L.I. Barabash, M.I. Starchik, V. K. Dubovoy, et al., Radiation hardness of silicon detectors based on pre-irradiated silicon, Nucl. Instr. Meth. A 568 (2006) 78–82.
[6] S.J. Moloi, M. McPherson, The current and capacitance response of radiation-damaged silicon PIN diodes, Phys. B 404 (21) (2009) 3922–3929.
[7] M. Msimanga, M. McPherson, Diffusion characteristics of gold in silicon and electrical properties of silicon diodes used for developing radiation-hard detectors, Mater. Sci. Eng., B 127 (2006) 47–54.
[8] S. Terzo, et al., Radiation hard silicon particle detectors for HL-LHC—RD50 status report, Nucl. Instr. Meth. Phys. Res. A 845 (2017) 177–180.
[9] M.K. Parida, S.T. Sundari, V. Sathia Moorthy, S. Sivakumar, Current–voltage characteristics of silicon PIN diodes irradiated in KAMINI nuclear reactor, Nucl. Instr. Meth. Phys. Res. A 568 (2018) 7129–7137.
[10] M. Schulz, Determination of deep trap levels in silicon using ion-implantation and CV-measurements, Appl. Phys. 4 (3) (1974) 225–236.
[11] H. Pettersson, H.G. Grimmeiss, L. Tilly, K. Schmalz, H. Kerkow, Electrical and optical characterization of niobium-related centres in silicon, Semicond. Sci. Technol. 8 (7) (1993) 1247–1252.
[12] M.L. Polignano, D. Codegoni, G. Borionetti, F. Bonoli, J. Brivio, S. Greco, A. Marino, P. Monge, I. Patoprsta, V. Privitera, C. Riva, Niobium contamination in silicon, ECS Transaction 33 (11) (2010) 133–144.
[13] K. Watanabe, C. Munakata, Recombination lifetime in a gold-doped p-type silicon crystal, Semicond. Sci. Technol. 8 (2) (1993) 230–235.
[14] Y.K. Kwon, T. Ishikawa, H. Kuwano, Properties of platinum-associated deep levels in silicon, J. Appl. Phys. 61 (1987) 1055-.
[15] M. McPherson, Fermi level pinning in irradiated silicon considered as a relaxation-like semiconductor, Phys. B 344 (1-4) (2004) 52–57.
[16] S.J. Moloi, M. McPherson, Current–voltage behavior of Schottky diodes fabricated on p-type silicon for radiation hard detectors, Phys. B 404 (2009) 2251–2258.
[17] S.M. Sze, Physics of Semiconductor Devices, second ed., Wiley, NewYork, 1981.
[18] D.K. Schroder, Semiconductor Material and Device Characterization, third ed., Wiley, NewYork, 2006.
[19] B.G. Streetman, Solid State Electronic Devices, third ed., Prentice Hall, London, 1990.
[20] Ş. Karataş, Ş. Altındal, Analysis of I-V characteristics on Au/n-type GaAs Schottky structures in wide temperature range, Mater. Sci. Eng. 122 (2) (2005) 133–139.

[21] V.E. Gora, F.D. Auret, H.T. Danga, S.M. Tunhuma, C. Nyamhere, E. Igumbor, A. Chawanda, Barrier height inhomogeneities on Pd/n-4H-SiC Schottky diodes in a wide temperature range, Mater. Sci. Eng., B 247 (2019), 114370.
[22] T. Tunç, Ş. Altindal, İ. Uslu, İ. Dökme, H. Uslu, Temperature dependent current–voltage (I–V) characteristics of Au/n-Si (111) Schottky barrier diodes with PVA (Ni, Zn-doped) interfacial layer, Mater. Sci. Semicond. Process. 14 (2) (2011) 139–145.
[23] J. Osvald, K. Hricovini, G. Le Lay, V.Y. Aristov, Pb/Si (111)1X1-H Schottky barrier height, Fizika A 2 (1995) 191–197.
[24] Z.J. Horváth, M. Ádám, I. Szabó, M. Serényi, V.o. Van Tuyen, Modification of Al/Si interface and Schottky barrier height with chemical treatment, Appl. Surf. Sci. 190 (1-4) (2002) 441–444.
[25] M. Siad, A. Keffous, S. Mamma, Y. Belkacem, H. Menari, Correlation between series resistance and parameters of Al/n-Si and Al/p-Si Schottky barrier diodes, Appl. Surf. Sci. 236 (1-4) (2004) 366–376.
[26] R. Singh, S.K. Arora, D. Kanjilal, Swift heavy ion irradiation induced modification of electrical characteristics of Au/n-Si Schottky barrier diode, Mater. Sci. Semicond. Process. 4 (5) (2001) 425–432.
[27] Ö. Güllü, F. Demir, F.E. Cimilli, M. Biber, γ-Irradiation-induced changes at the electrical characteristics of Sn/p–Si Schottky contacts, Vacuum 82 (8) (2008) 789–793.
[28] P.L. Hanselaer, W.H. Laflere, R.L. Meirhaeghe, F. Cardon, The influence of a HF and an annealing treatment on the Barrier Height of p- and n- type Si MIS structures, Appl. Phys. A 39 (2) (1986) 129–133.
[29] H. Çetin, B. Şahin, E. Ayyildiz, A. Türüt, Ti/p-Si Schottky barrier diodes with interfacial layer prepared by thermal oxidation, Phys. B 364 (1-4) (2005) 133–141.
[30] S. Krishnan, G. Sanjeev, M. Pattabi, Electron irradiation effects on the Schottky diode characteristics of p-Si, Nucl. Instr. Meth. B 266 (4) (2008) 621–624.
[31] S.K. Cheung, N.W. Cheung, Extraction of Schottky diode parameters from forward current-voltage characteristics, Appl. Phys. Lett. 49 (2) (1986) 85–87.
[32] T. Kılıçoğlu, Effect of an organic compound (Methyl Red) interfacial layer on the calculation of characteristic parameters of an Al/Methyl Red/p-Si sandwich Schottky barrier diode, Thin Solid Films 516 (6) (2008) 967–970.
[33] I. Missoum, Y.S. Ocak, M. Benhaliliba, C.E. Benouis, A. Chaker, Microelectronic properties of organic Schottky diodes based on MgPc for solar cell applications, Synth. Met. 214 (2016) 76–81.
[34] A. Kaya, E. Marıl, Ş. Altındal, İ. Uslu, The comparative electrical characteristics of Au/n-Si (MS) diodes with and without a 2% graphene cobalt-doped $Ca_3Co_4Ga_{0.001}O_x$ interfacial layer at room temperature, Microelectron. Eng. 149 (2016) 166–171.
[35] V.N. Brudnyi, S.N. Grinyaev, V.E. Stepanov, Local neutrality conception: Fermi level pinning in defective semiconductors, Phys. B 212 (1995) 429–435.
[36] Y. Munikrishna Reddy, R. Padmasuvarna, T. Lakshmi Narasappa, P. Sreehith, R. Padma, L. Dasaradha Rao, V. Rajagopal Reddy, Effect of annealing temperature on the electrical, structural and surface morphological properties of Ru/Ti Schottky contacts on n-type InP, Superlattice and Microstructures 86 (2015) 280–291.
[37] M. Higashiwaki, K. Konishi, K. Sasaki, K. Goto, K. Nomura, et al., Temperature-dependent capacitance–voltage and current–voltage characteristics of Pt/Ga2O3 (001) Schottky barrier diodes fabricated on *n*—Ga_2O_3 drift layers grown by halide vapor phase epitaxy, Appl. Phys. Lett. 108 (13) (2016) 133503.
[38] T. Asar, B. Korkmaz, S. Ozcelik, Effects of platinum doping on the structural and electrical properties of SnO_2 thin film, J. Exp. Nanosci. 11 (16) (2016) 1285–1306.
[39] S. Karatas, A. Turut, Electrical properties of Sn/p-Si (MS) Schottky barrier diodes to be exposed 60Co γ-ray source, Nucl. Instr. Meth. Phys. Res. A 566 (2006) 584–589.